Advanced plasma drift velocity calculation technique

Alex Koloskov, A. Kashcheyev, P.T. Jayachandran

Department of Physics, University of New Brunswick, Fredericton, NB, Canada

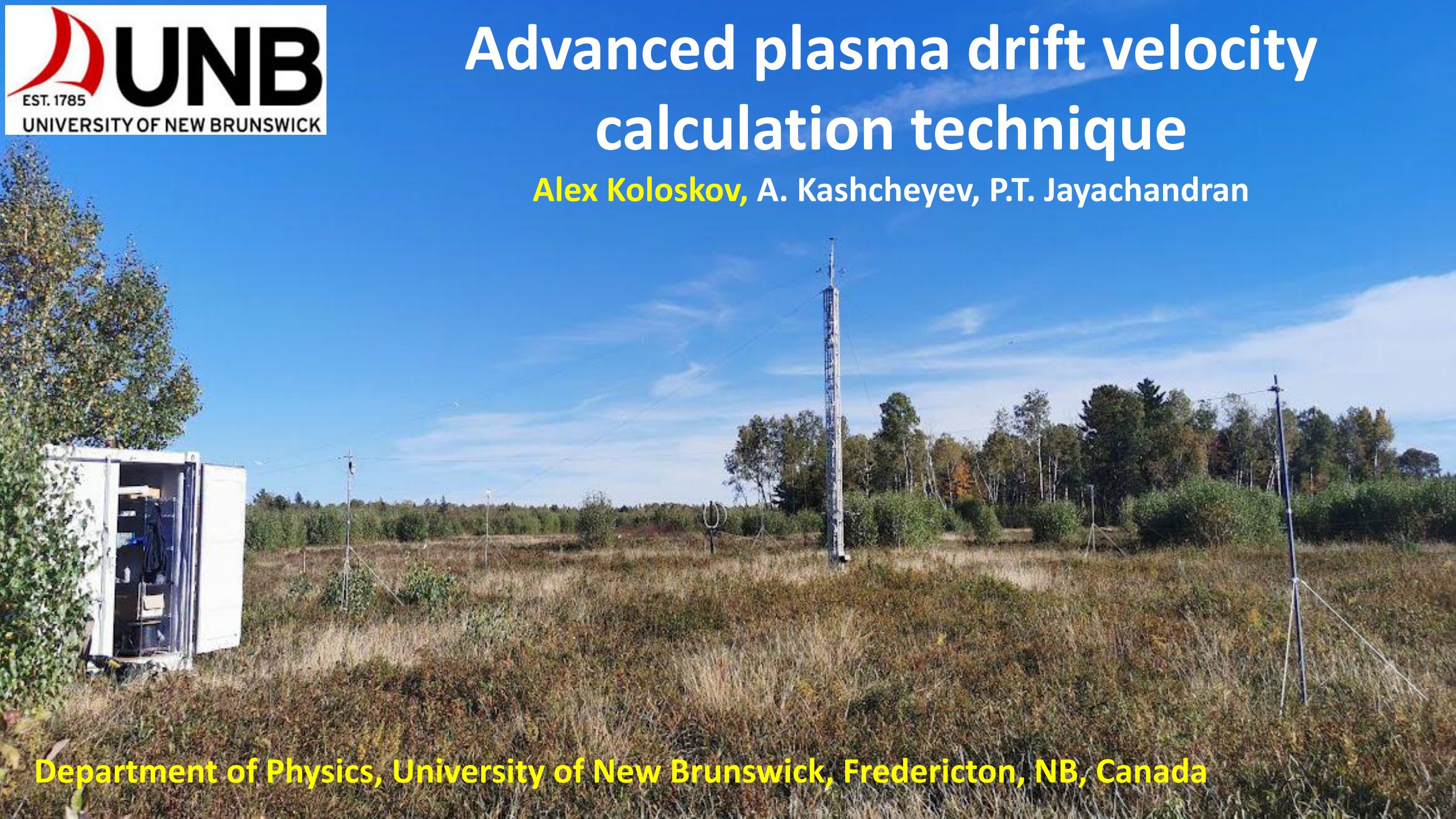

The **Canadian Advanced Digital Ionosonde (CADI)** is a low cost, state of the art, flexible, full featured ionosonde ideal for both routine ionospheric monitoring and research.

Adapted from https://www.sil.sk.ca/content/cadi

Digisonde-Portable-Sounder-4D (DPS4D) developed by Lowell Digisonde International measures all parameters of the ionospherically reflected HF radio signals, and provie automatic scaling of ionograms.

Adapted from https://digisonde.com/digisonde.html

Assuming uniform ionospheric motion in the signal illumination area and using AOA and Doppler shift that produce so called Skymap, three components (N-S, E-W, and vertical) of the ionospheric plasma drift are determined.

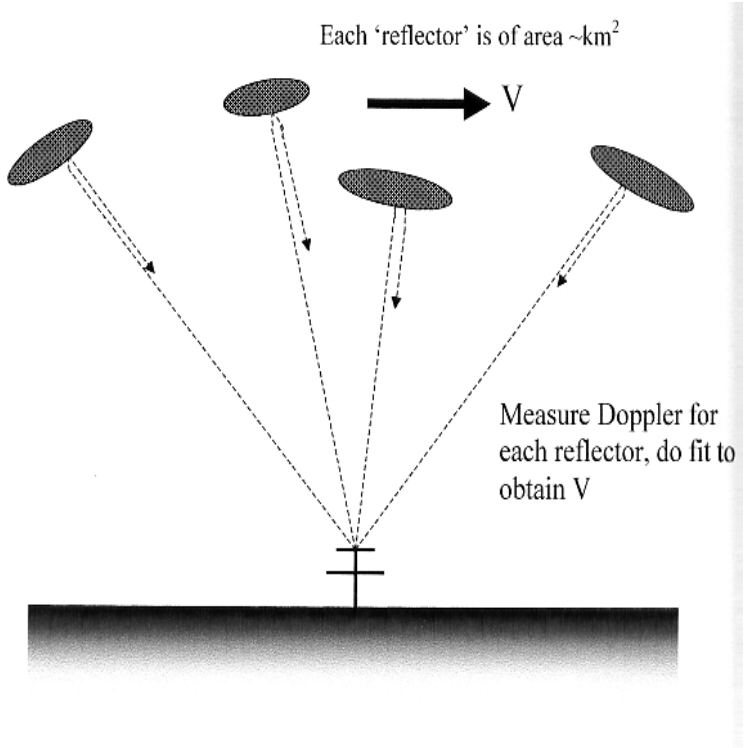

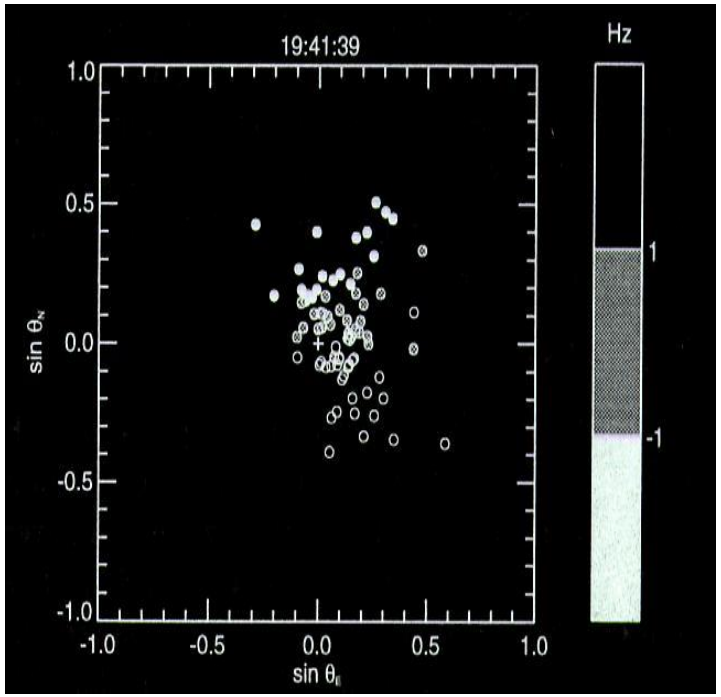

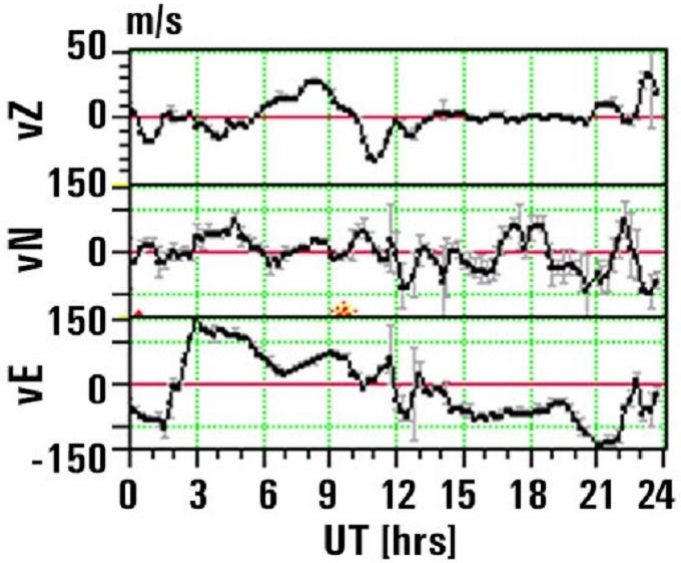

Adapted from http://chain.physics.unb.ca/chain/pages/cadi/

Adapted from: Morris, R. J., D. P. Monselesan, M. R. Hyde, A. M. Breed, and P. J. Wilkinson (2004), *Southern polar cap DPS and CADI ionosonde measurements: 2. F-region drift comparison*, ***Adv. Space Res.,*** 33(6), 937–942.

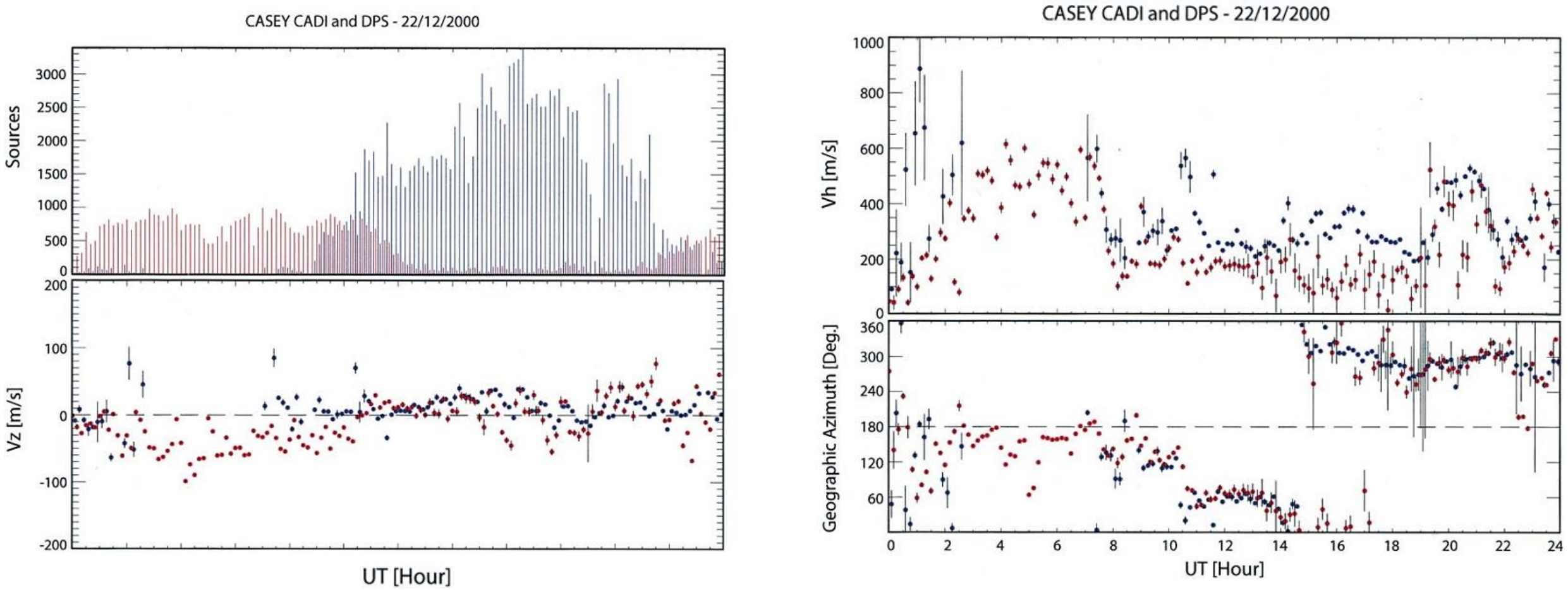

Fig. 2. **DPS (blue)** and **CADI (red)** F-region drift parameters observed at Casey on 22 December 2000 [sources, number of returned echoes; Vz, vertical drift velocity; Vh, horizontal drift velocity; and geographic azimuth].

Automatic drift data processing from collocated CADI and Digisonde collected in Antarctica **sometimes showed different results**. Measurements at polar cap station Casey (110.5°E, 66.3°S geographic, 81.0°S magnetic)

Modular Digital Ionospheric Sounder (MODIS)

- **Low-powered**, **low-cost** HF system
- **Modular concept** and **versatility**: Capable of functioning both as an **active and passive ionosonde**, multichannel coherent **HF receiver,** and a **riometer**
- Designed for operation in **hostile and remote environments**, such as Arctic locations. For example, the Canadian High Arctic Ionospheric Network.

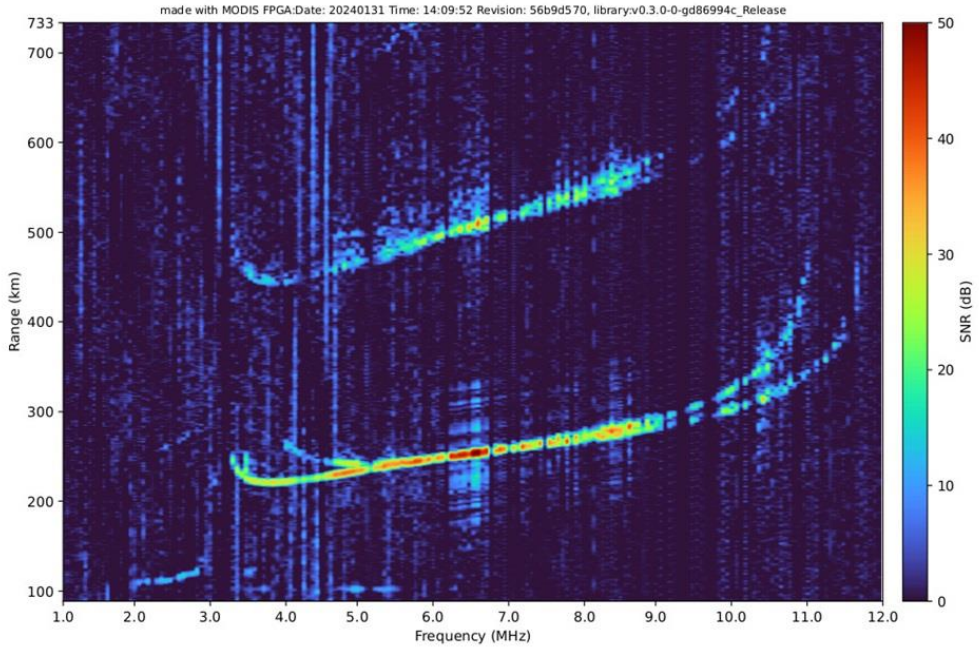

STEP 1: Doppler interferometry technique angles of arrival (AoA) calculations

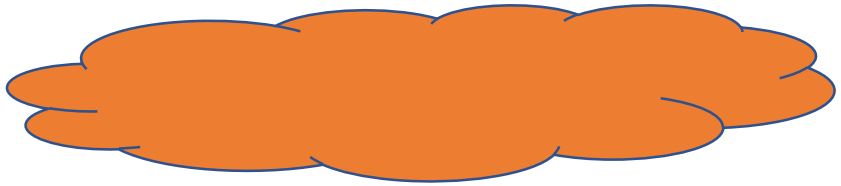

STEP 1: Doppler interferometry technique angles of arrival (AoA) calculations

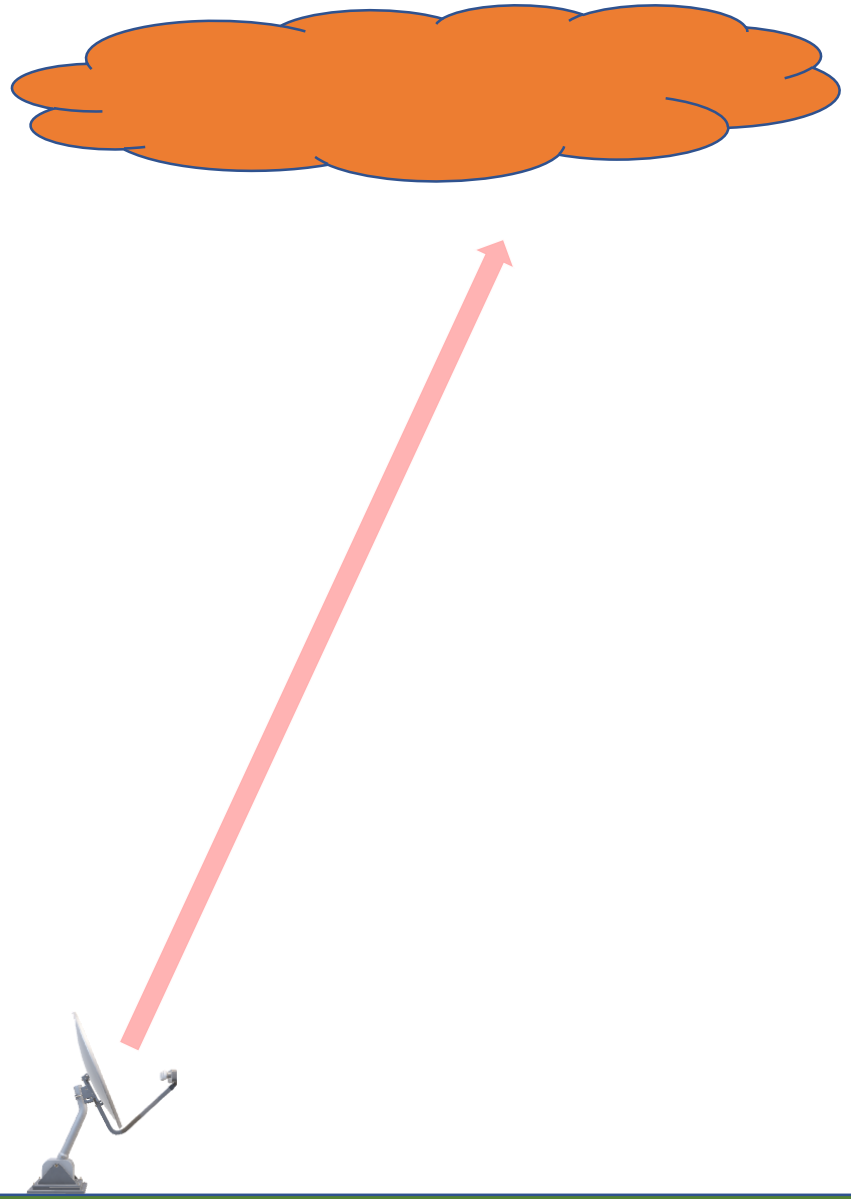

STEP 1: Doppler interferometry technique angles of arrival (AoA) calculations

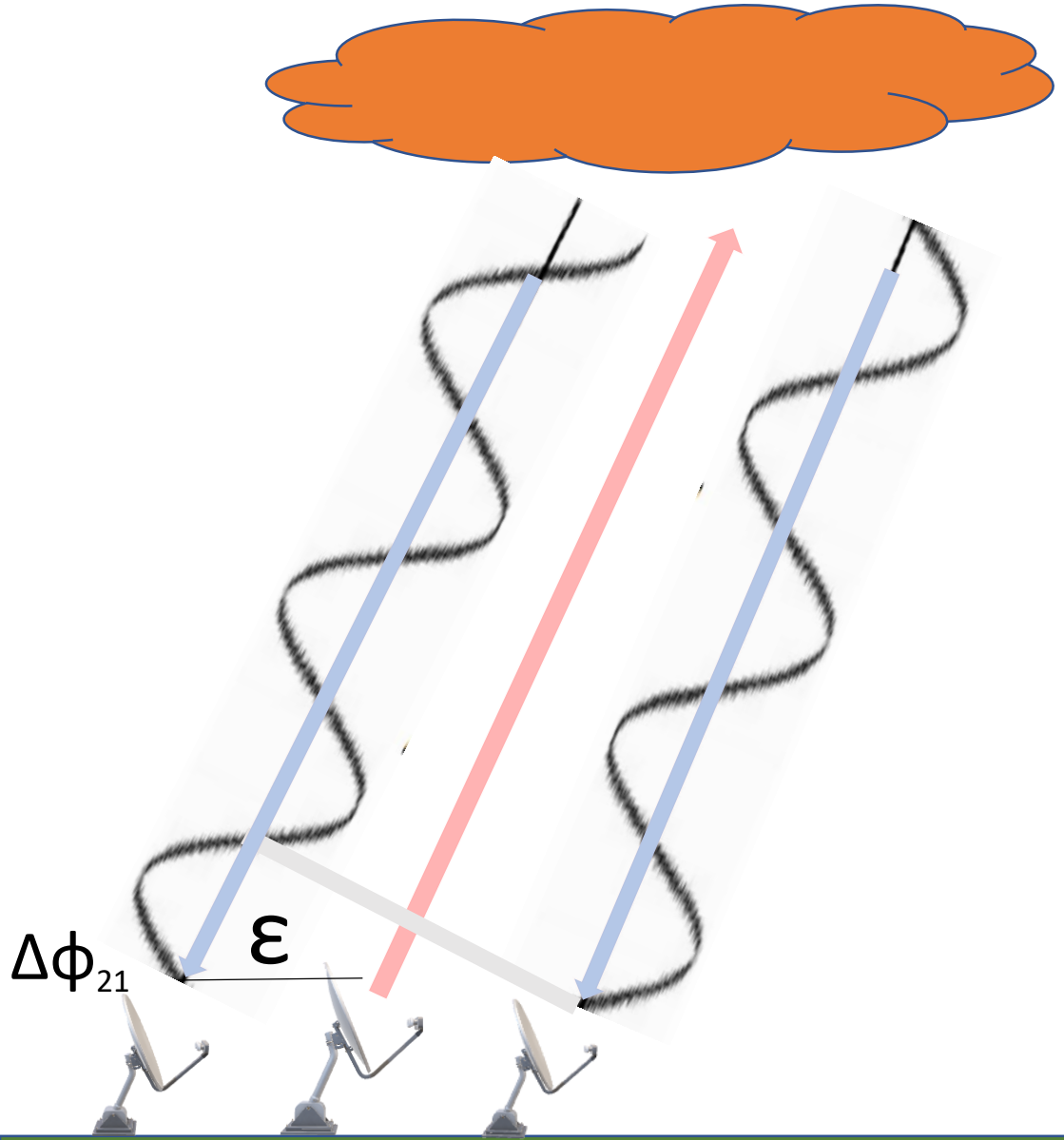

STEP 1: Doppler interferometry technique angles of arrival (AoA) calculations

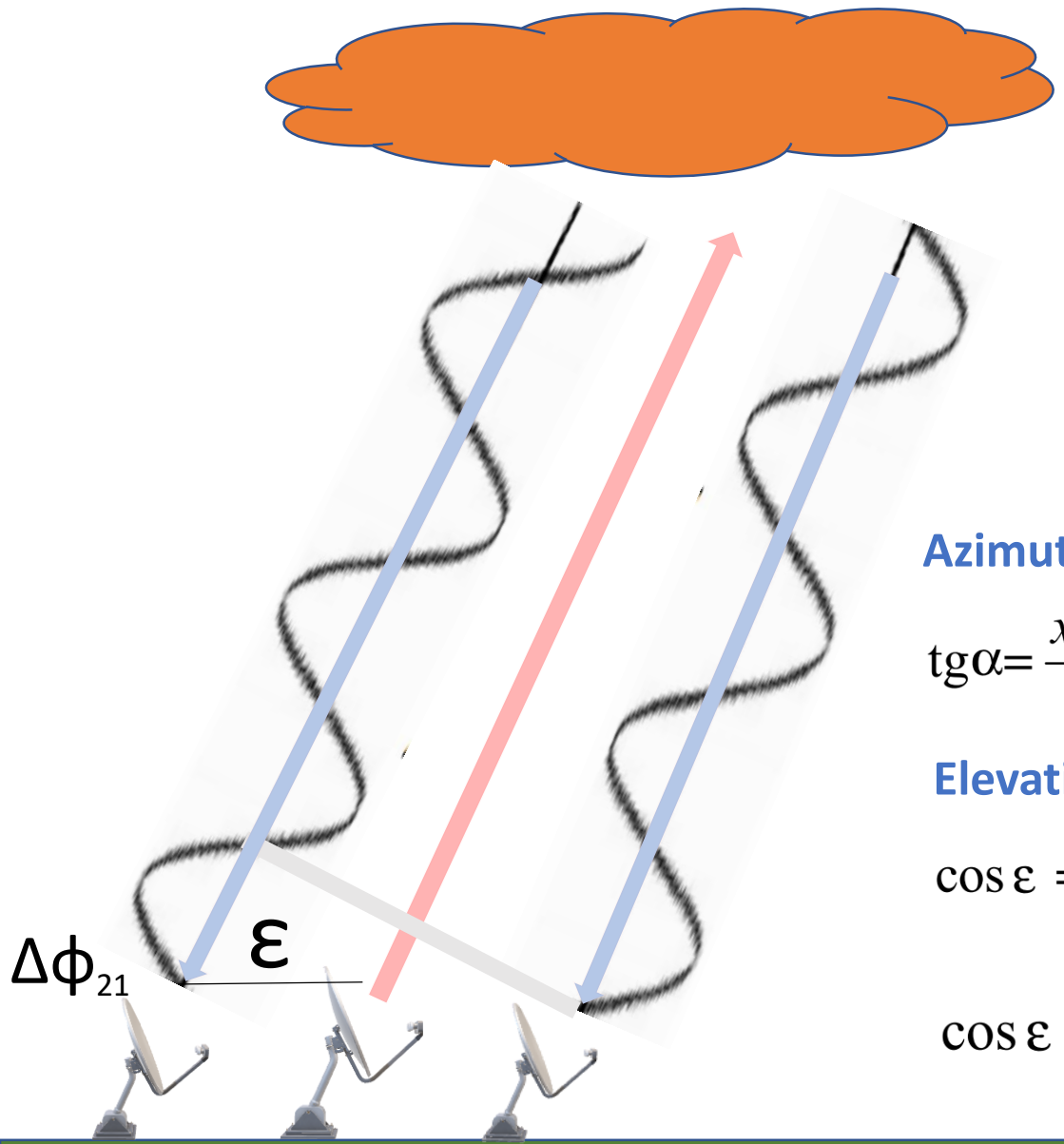

Calculating the Angle of Arrival (AoA) require a minimum of three spatially separated Rx antennas. If the antennas are positioned at locations 1, 2, and 3, and we have determined the phase differences from measurements:

$$\Delta\varphi_{2-1} = \varphi_2 - \varphi_1 \qquad \Delta\varphi_{3-1} = \varphi_3 - \varphi_1$$

AoA (α, ε) can be determined using the formulas:

Azimuth:

$$\mathrm{tg}\alpha = \frac{x_2\Delta\varphi_{3-1} - x_3\Delta\varphi_{2-1}}{y_3\Delta\varphi_{2-1}},$$

Elevation angle:

$$\cos\varepsilon = \frac{\Delta\varphi_{3-1}}{k(x_3\cos\alpha + y_3\sin\alpha)},$$

$$\cos\varepsilon = \frac{\Delta\varphi_{2-1}}{kx_2\cos\alpha}$$

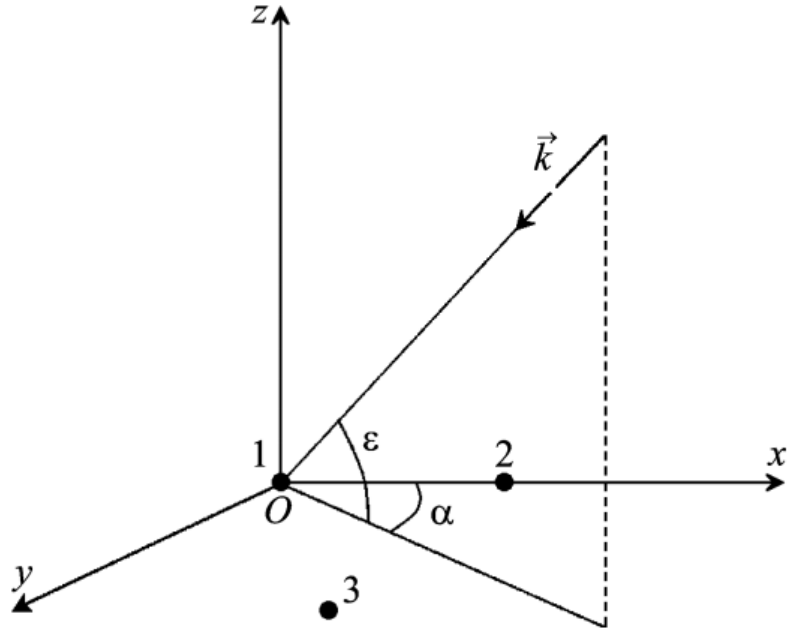

Drift velocities calculation

SkyMaps of radial velocity

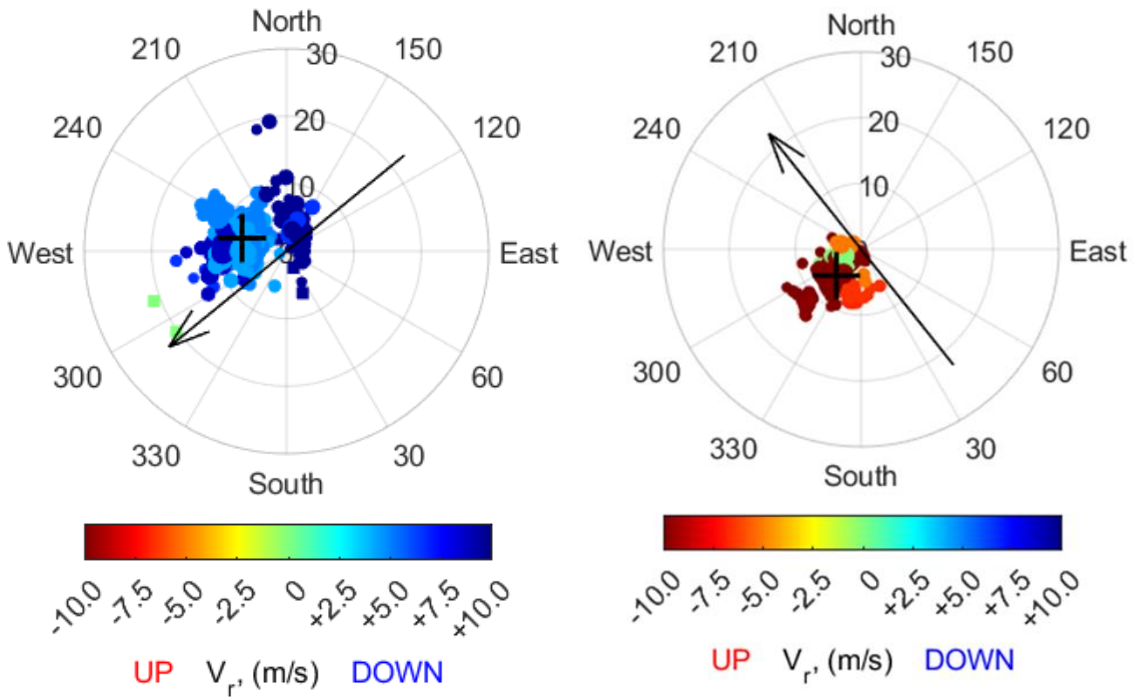

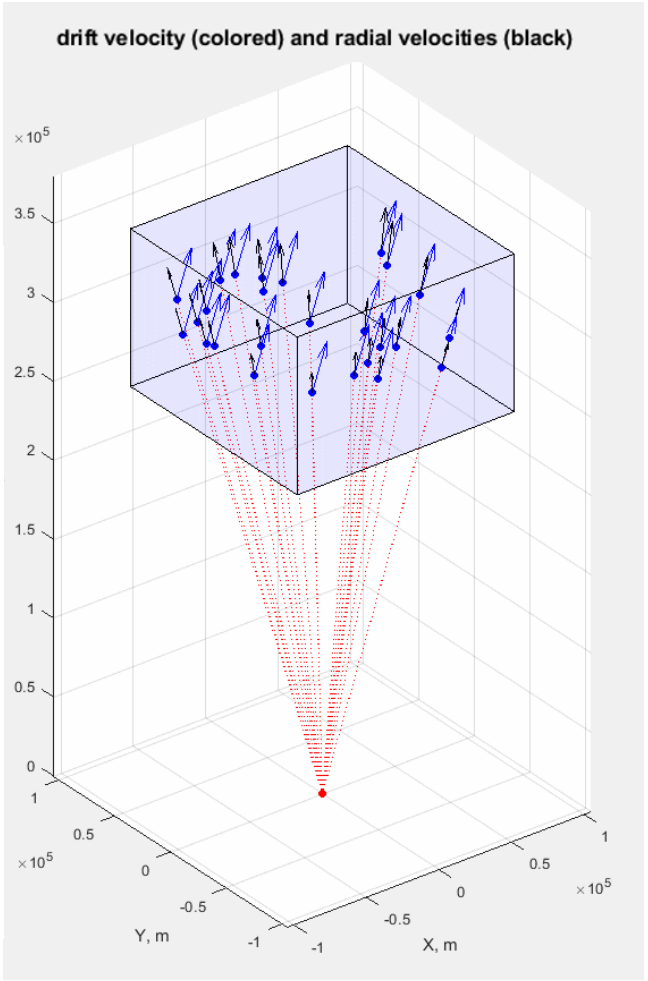

(Rx_1, Rx_2, Rx_3) -> $F_{D1} = F_{D2} = F_{D3}$

Radial velocities from DFS:

$$V_r^{/} = \frac{1}{2}\frac{F_D c}{f}$$

Minimizing the sum of the squares of the residuals

we determine from observations:

$$V_{ri} \rightarrow (V_{xi}, V_{yi}, V_{zi}), \qquad i = 1 \ldots n$$

we assume that the direction and magnitude of the drift velocity

$$(\boldsymbol{V_{dx}}, \boldsymbol{V_{dy}}, \boldsymbol{V_{dz}})$$

$$F = \min \left\{ \sum_{i=1}^{n} (\boldsymbol{V_{dx}} - V_{xi})^2 + (\boldsymbol{V_{dy}} - V_{yi})^2 + (\boldsymbol{V_{dz}} - V_{zi})^2 \right\}$$

are the same inside the reflecting volume

Generalized drift velocity analysis

Investigations of high-latitude convections indicated that the motion of plasma within the reflected volume may not be uniform. In order to correctly identify the main velocity components within the volume ***combination*** analysis may be used to develop **a velocity field distribution** in which **all velocity components** within a reflected region are resolved. Calculation of Vd_{Xi}, Vd_{Yi}, Vd_{Zi} ***(I = 1..N)*** for complete set of *N combinations*. The final resultant distribution of velocities will represent a velocity field in which the most frequent specific velocities correspond to the actual drift velocities.

$$d_i = \frac{1}{\pi}\boldsymbol{k}_i \cdot \boldsymbol{v}_D = \frac{2}{\lambda} v_{\mathrm{los},i} \quad \boldsymbol{v}_D = (v_x,\ v_y,\ v_z) \quad i = 1, 2, 3.$$

$$\frac{1}{2}\lambda d_i = v_x \cos\phi_i \sin\theta_i + v_i \sin\phi_i \sin\theta_i + v_z \cos\theta_i$$

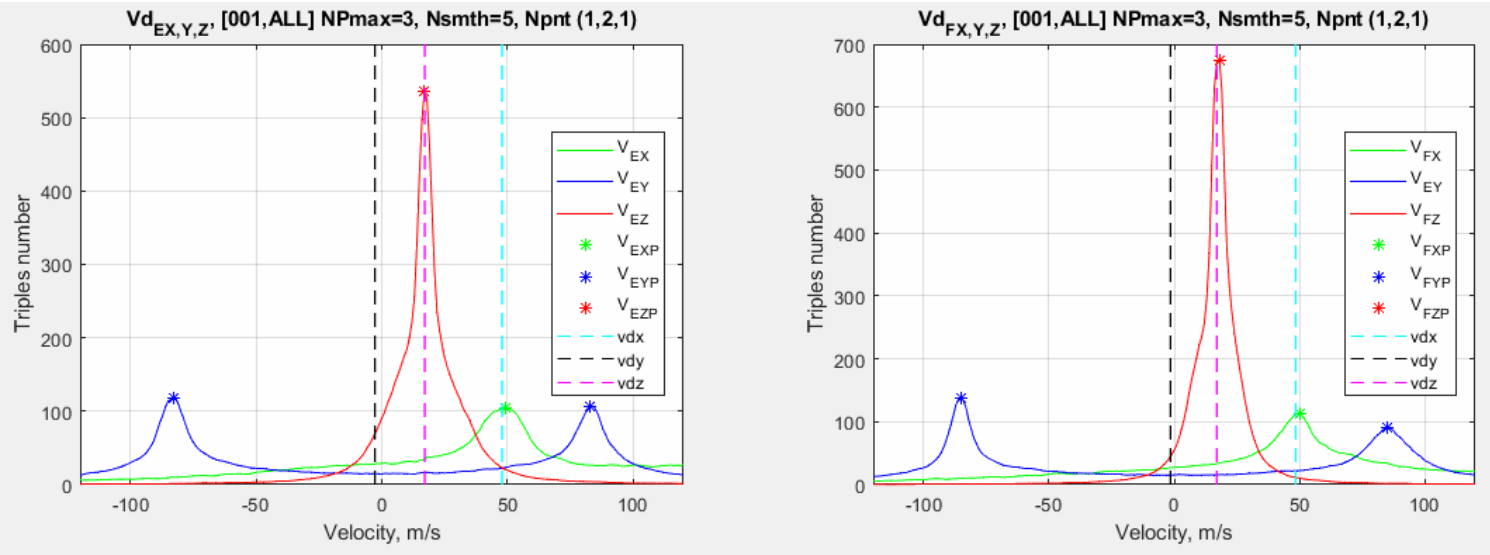

The advantages of the algorithm:

- The ability to determine **multiple speed vectors**
- solution for an **arbitrary locations of receiving antennas,** including those spaced vertically

Software for Sky Map and Drift Velocity calculation

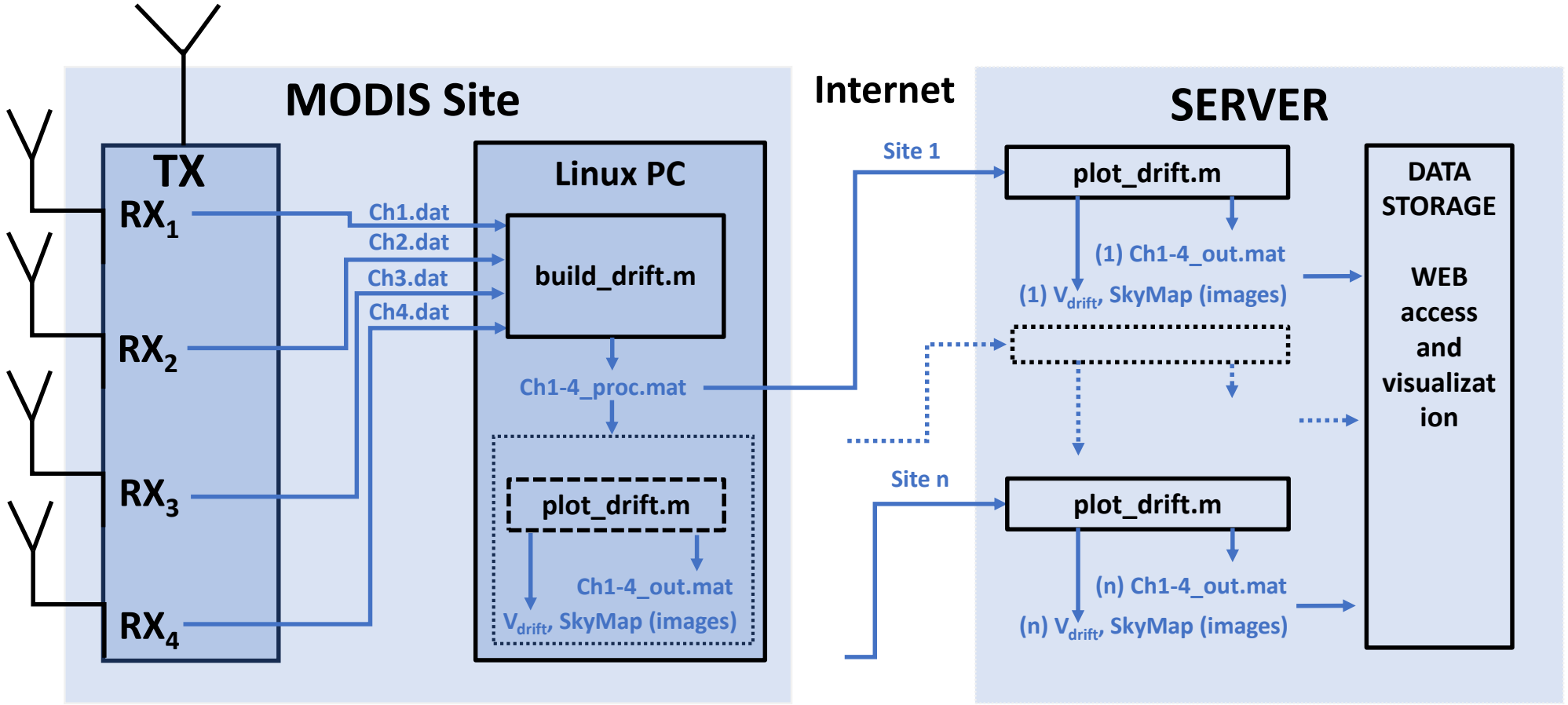

Field tests of the algorithm were conducted using the CADI ionosonde antenna system at a mid-latitude near Blissville, NB. Since we currently do not have data from collocated ionosondes for validating the results obtained in Blissville, they were compared with data from a digisonde in Millstone Hill, Massachusetts, USA.

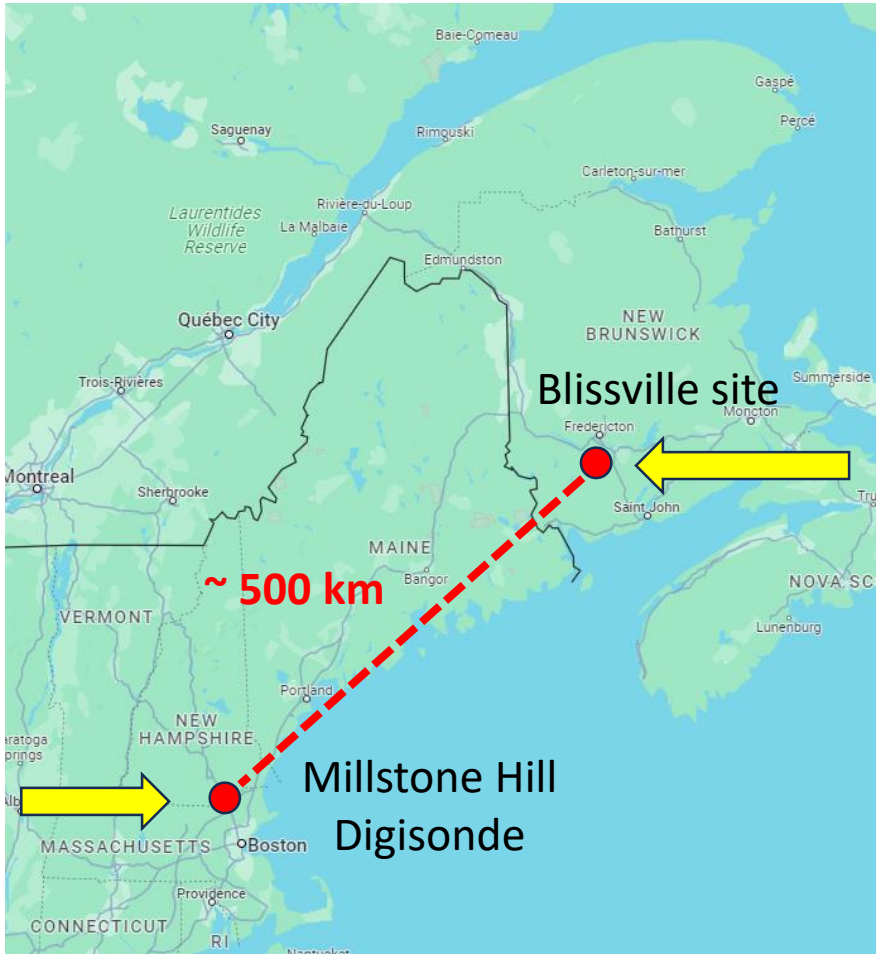

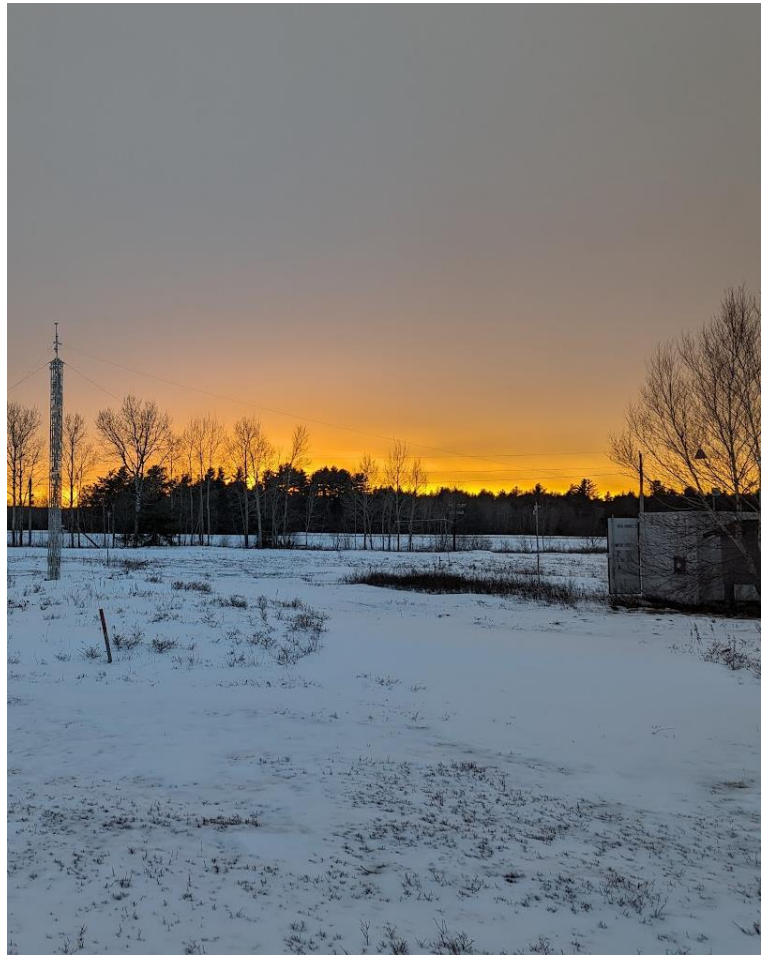

Future observations are planned in the high-latitude regions, including a site in Resolute Bay, NU and other sites of Canadian High Arctic Ionospheric Network (CHAIN).

29 Oct – 03 Nov 2022 Blissville, preliminary comparison with Millstone Hill Digisonde

29 Oct – 03 Nov 2022, V_{drift}

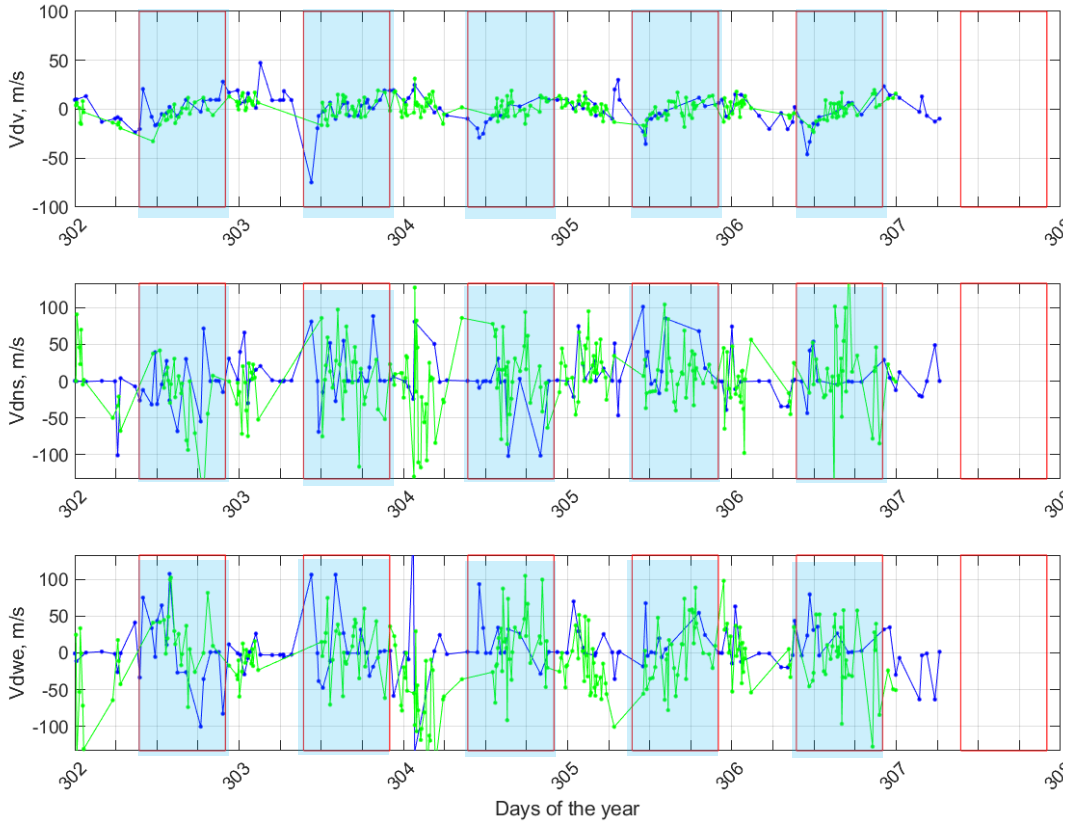

Daily averaged, V_{drift}

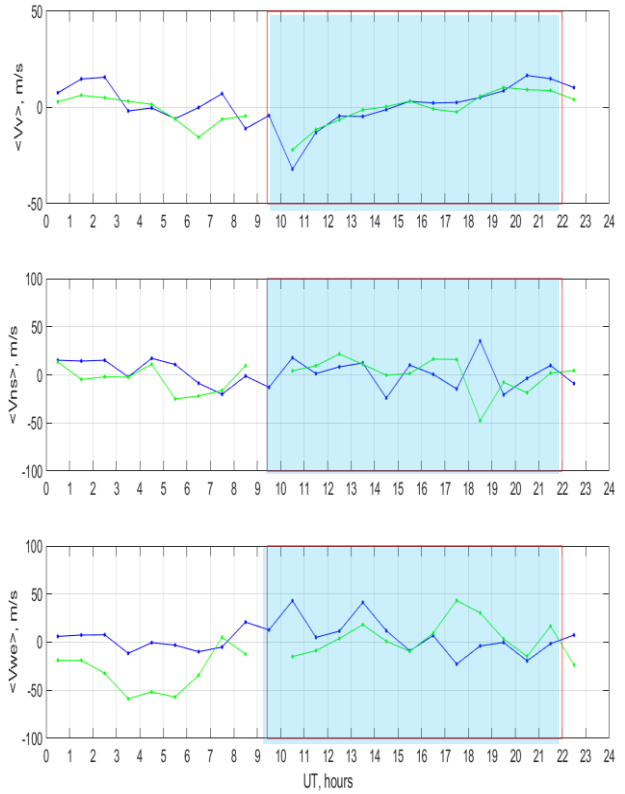

Hist, V_{dv}

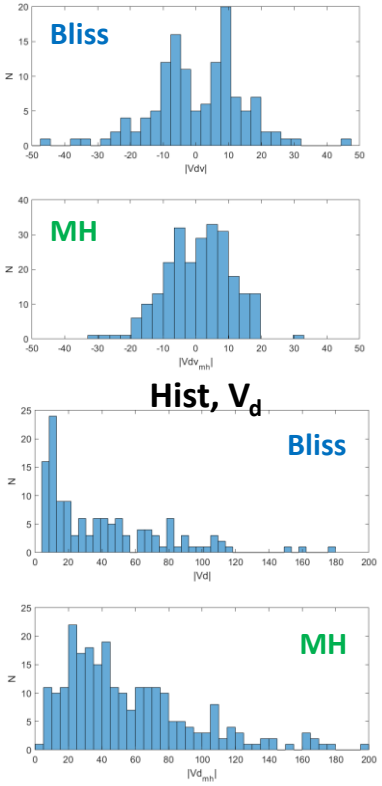

Hist, V_d

Factors affecting the accuracy of drift velocity calculation

- **Low DFS resolution (T~5.8 sec, dF step ~ 0.17 Hz for standard drift sounding regime)**

$F_{sounding}$(E) = 2.744 MHz, $F_{sounding}$(F) = 6.044 MHz

T s, dF Hz	5.8 s / 0.17 Hz			20 s / 0.05 Hz			30 s / 0.033 Hz		
ΔΘ	15°	20°	30°	15°	20°	30°	15°	20°	30°
dV_Z(E)		9.3 m/s			2.8 m/s			1.9 m/s	
dV_Z(F)		4.2 m/s			1.3 m/s			0.8 m/s	
dV_{HORIZ}(E)	35.9 m/s	27.2 m/s	18.6 m/s	10.8 m/s	8.2 m/s	5.6 m/s	7.2 m/s	5.4 m/s	3.7 m/s
dV_{HORIZ}(F)	16.2 m/s	12.2 m/s	8.4 m/s	4.9 m/s	3.7 m/s	2.5 m/s	3.2 m/s	2.4 m/s	1.7 m/s

- **Drift velocities for the E and F regions may differ. Therefore, it is reasonable to calculate the drift velocity (Vd) separately for each region. For each region, quality control must be performed on the acquired data before calculating drift velocities.**

Additional phase shifts in perpendicular antennas due to off-vertical propagation

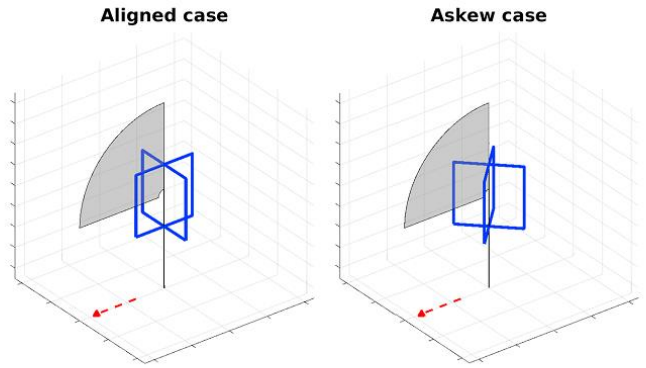

Figure 6. Diagram of a pair of orthogonal magnetic loop receive antennas (shown in blue) and expected incident direction of OIS signals (gray arc). The dashed red line indicates the direction of the OIS transmitter. (left) Aligned case. (right) Askew case.

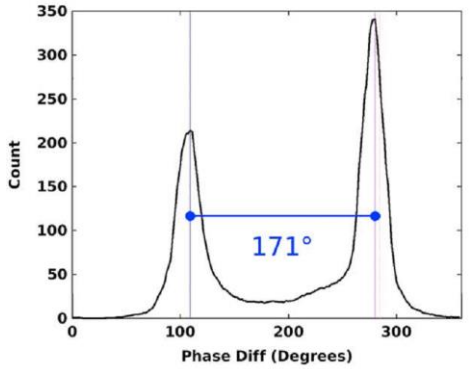

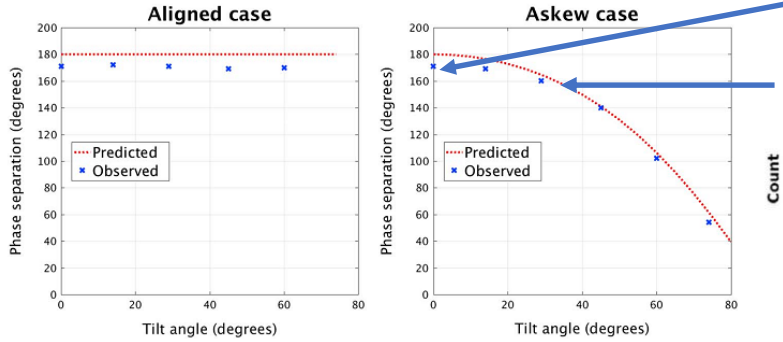

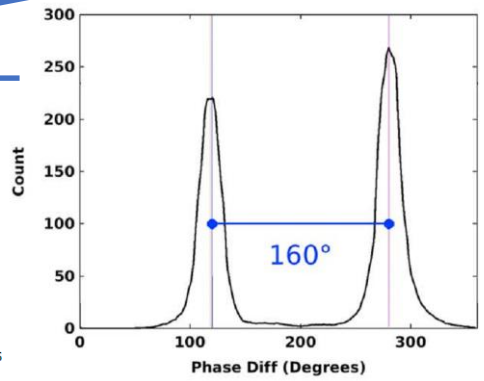

Figure 11. Predicted and observed phase separation versus tilt angle. (left) Results for aligned case. (right) Results askew case.

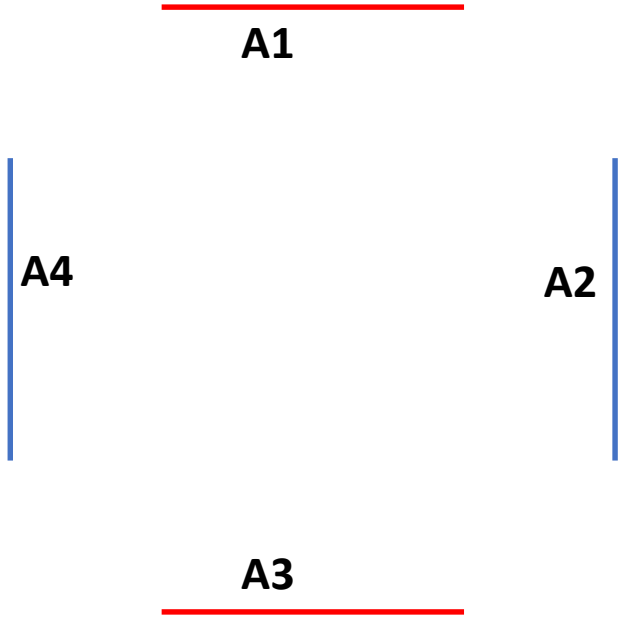

ϕ - the **antenna's tilt axis offset** (angle between dipole antenna orientation and azimuth of tilt)
θ - the **rotation angle** (zenith angle)
α - the phase separation () is equal to:

$$\cos\left(\frac{\alpha}{2}\right) = \frac{\sin\phi\cos\phi\sin^2\theta}{\sqrt{\left(\cos^2\phi + \cos^2\theta\sin^2\phi\right)\left(\sin^2\phi + \cos^2\theta\cos^2\phi\right)}}.$$

Harris, T. J., Cervera, M. A., Pederick, L. H., & Quinn, A. D. (2017). Separation of O/X polarization modes on oblique ionospheric soundings, Radio Science, 52, 1522–1533. https://doi.org/10.1002/2017RS006280).

Additional phase shifts in perpendicular antennas due to off-vertical propagation

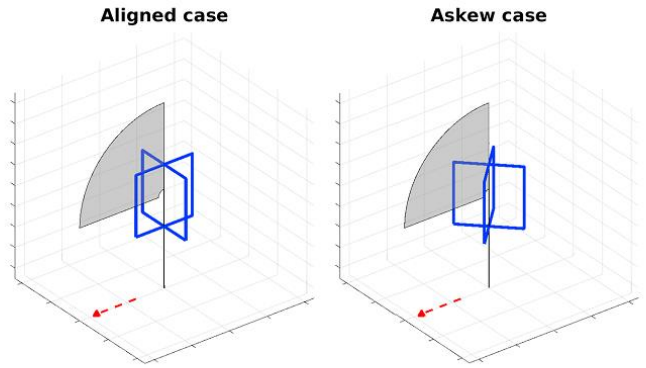

Figure 6. Diagram of a pair of orthogonal magnetic loop receive antennas (shown in blue) and expected incident direction of OIS signals (gray arc). The dashed red line indicates the direction of the OIS transmitter. (left) Aligned case. (right) Askew case.

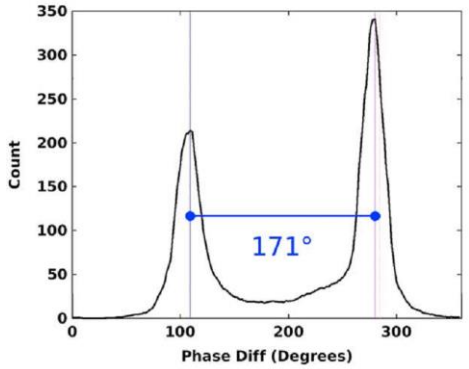

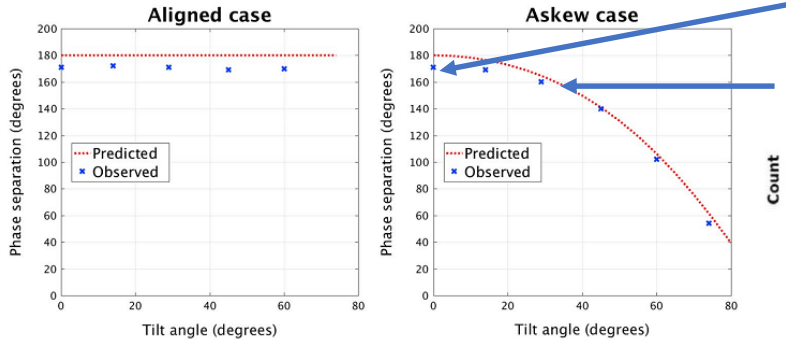

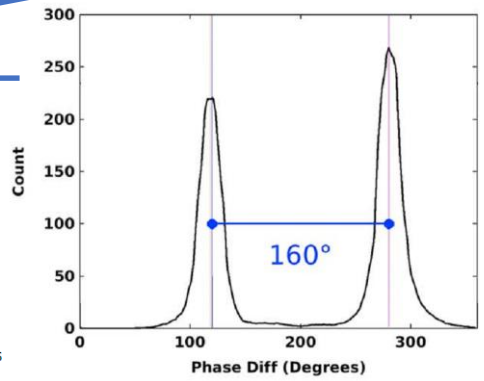

Figure 11. Predicted and observed phase separation versus tilt angle. (left) Results for aligned case. (right) Results askew case.

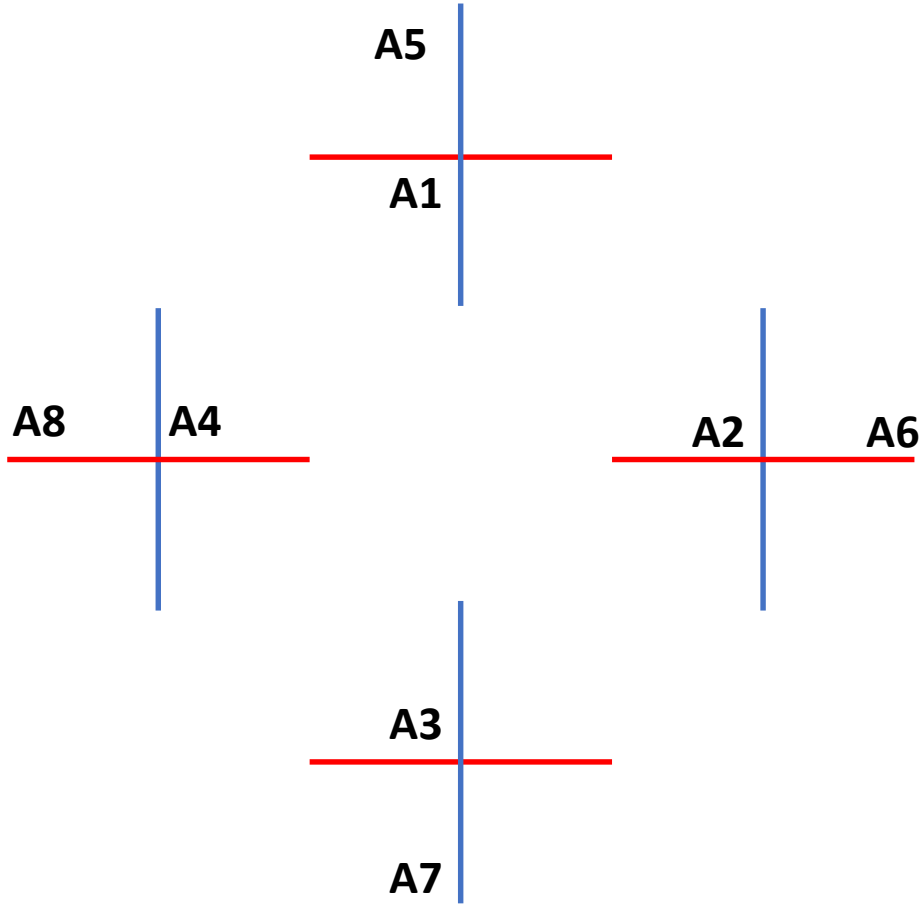

ϕ - the **antenna's tilt axis offset** (angle between dipole antenna orientation and azimuth of tilt)
θ - the **rotation angle** (zenith angle)
α - the phase separation () is equal to:

$$\cos\left(\frac{\alpha}{2}\right) = \frac{\sin\phi\cos\phi\sin^2\theta}{\sqrt{\left(\cos^2\phi + \cos^2\theta\sin^2\phi\right)\left(\sin^2\phi + \cos^2\theta\cos^2\phi\right)}}.$$

Harris, T. J., Cervera, M. A., Pederick, L. H., & Quinn, A. D. (2017). Separation of O/X polarization modes on oblique ionospheric soundings, Radio Science, 52, 1522–1533. https://doi.org/10.1002/2017RS006280).

We evaluated how additional phase differences affect the errors in determining the angles of arrival and drift velocity. These results will be used to develop recommendations for installing an ionosonde and conducting measurements at different latitudes and under different ionospheric conditions.

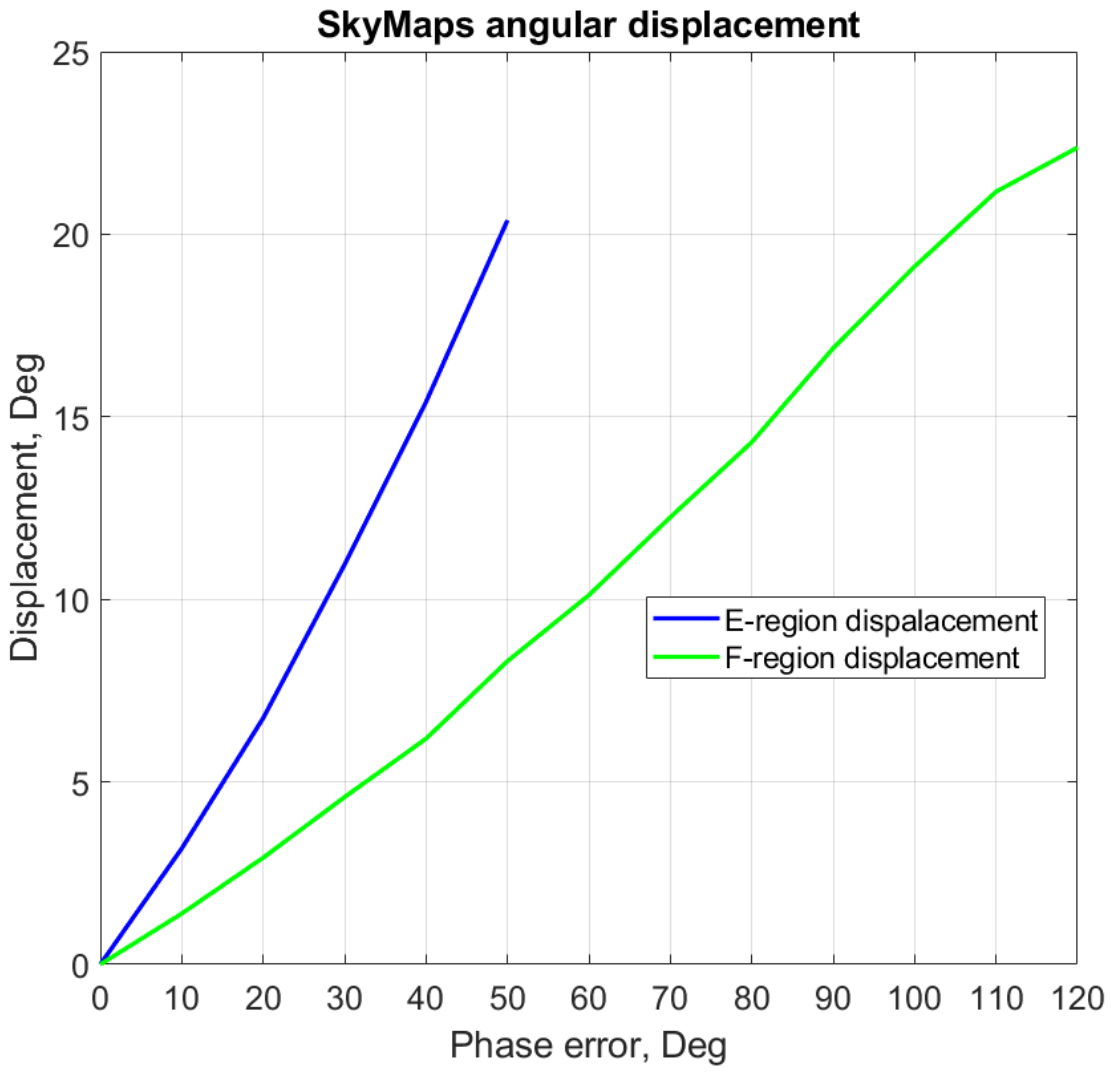

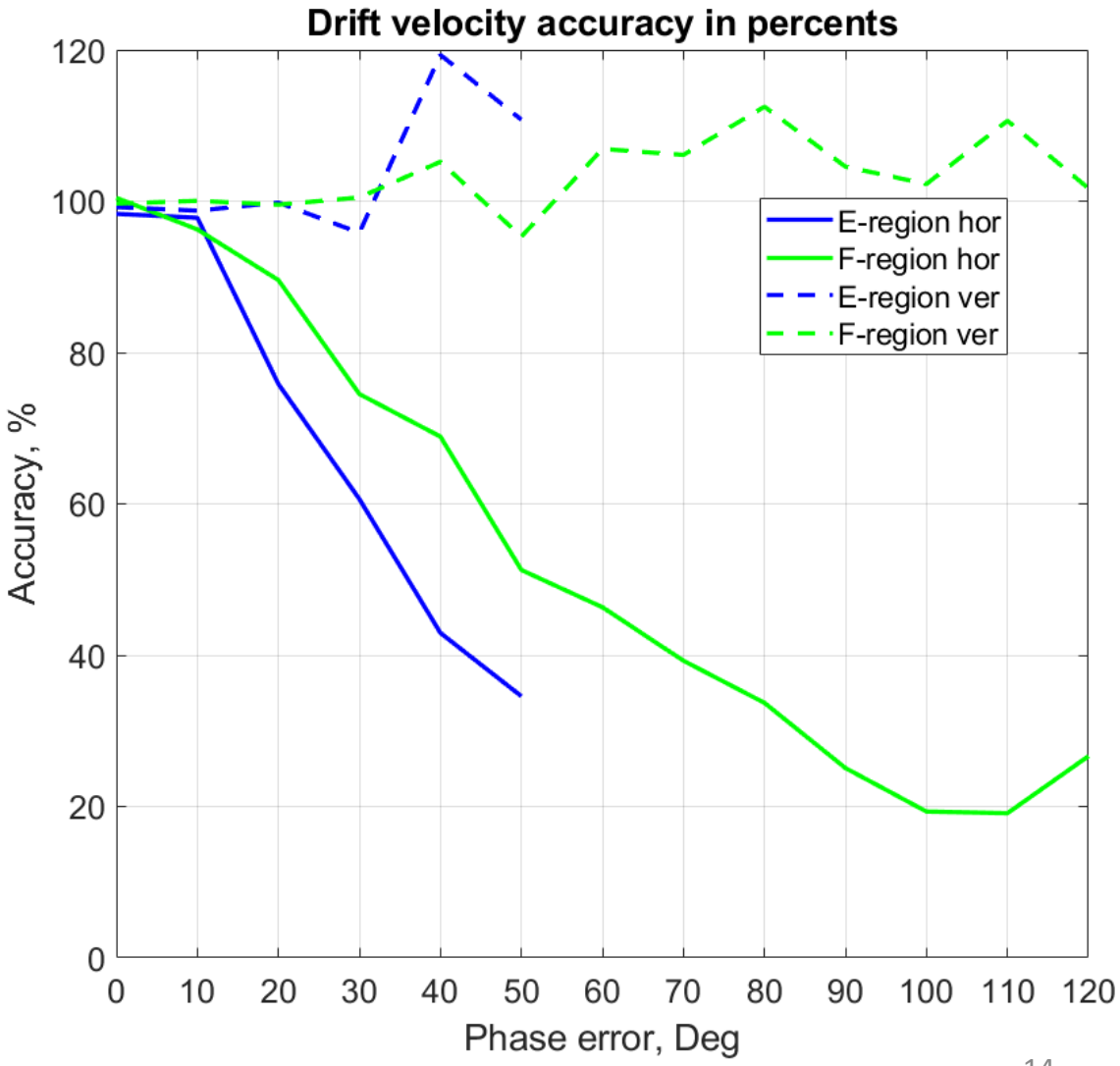

CONCLUSIONS

- An advance algorithm and software for plasma drift velocity calculation using digital ionosonde has been developed.
- The algorithm was validated by comparison with digisonde data.
- A simulation code was employed to estimate errors in the angle of arrival (AoA) and drift velocity (Vd) calculations.
- Various factors, including the resolution of Doppler frequency shift (dFd), size of the reflection area, and an additional phase shift due to different factors like off-vertical propagation were considered.
- Data processing for high-latitude regions will be carried out.
- The results will be compared with those obtained from CADI and other instruments.